

Efficient Parallel Simulations of Asynchronous Cellular Arrays

Boris D. Lubachevsky
bdl@bell-labs.com
Bell Laboratories
600 Mountain Avenue
Murray Hill, New Jersey

Abstract

A definition for a class of asynchronous cellular arrays is proposed. An example of such asynchrony would be independent Poisson arrivals of cell iterations. The Ising model in the continuous time formulation of Glauber falls into this class. Also proposed are efficient parallel algorithms for simulating these asynchronous cellular arrays. In the algorithms, one or several cells are assigned to a processing element (PE), local times for different PEs can be different. Although the standard serial algorithm by Metropolis, Rosenbluth, Rosenbluth, Teller, and Teller can simulate such arrays, it is usually believed to be without an efficient parallel counterpart. However, the proposed parallel algorithms contradict this belief proving to be both efficient and able to perform the same task as the standard algorithm. The results of experiments with the new algorithms are encouraging: the speed-up is greater than 16 using 25 PEs on a shared memory MIMD bus computer, and greater than 1900 using 2^{14} PEs on a SIMD computer. The algorithm by Bortz, Kalos, and Lebowitz can be incorporated in the proposed parallel algorithms, further contributing to speed-up.

1. Introduction

Simulation is inevitable in studying the evolution of complex cellular systems. Large cellular array simulations might require long runs on a serial computer. Parallel processing, wherein each cell or a group of cells is hosted by a separate processing element (PE), is a feasible method to speed up the runs. The strategy of a parallel simulation should depend on whether the simulated system is synchronous or asynchronous.

A *synchronous* system evolves in discrete time $t = 0, 1, 2, \dots$. The state of a cell at $t + 1$ is determined by the state of the cell and its neighbors at t and may explicitly depend on t and the result of a random experiment.

An obvious and correct way to simulate the system synchrony using a parallel processor is simply to mimic it by the executional synchrony. The simulation is arranged in rounds with one round corresponding to one time step and with no PE processing state changes of its cells for time $t + 1$ before all PEs have processed state changes of their cells for time t .

An *asynchronous* system evolves in continuous time. State changes at different cells occur asynchronously at unpredictable random times. Here two questions should be answered: (A) How to specify the asynchrony precisely? and (B) How to carry out the parallel simulations for the specified asynchrony?

Unlike the synchronous case, simple mimicry does not work well in the asynchronous case. When Geman and Geman [1], for example, employ executional *physical* asynchrony (introduced by different speeds of different PEs) to mimic the model asynchrony, the simulation becomes irreproducible with its results depending on executional timing. Such dependence may be tolerable in tasks other than simulation ([1] describes one such task, another example is given in [2]). In the task of simulation, however, it is a serious shortcoming as seen in the following example.

Suppose a simulationist, after observing the results of a program run, wishes to look closer at a certain phenomenon and inserts an additional ‘print’ statement into the code. As a result of the insertion, the executional timing changes and the phenomenon under investigation vanishes.

Ingerson and Buvel [3] and Hofmann [4] propose various reproducible computational procedures to simulate asynchronies in cellular arrays. However no uniform principle has been proposed, and no special attention to developing parallel algorithms has been paid. It has been observed that the resulting cellular patterns may depend on the computational procedure [3].

Two main results of this paper are: (I) a definition of a natural class of asynchronies that can be associated with cellular arrays and (II) efficient parallel algorithms to simulate systems in this class. The following properties specify the *Poisson asynchrony*, a most common member in the introduced class:

Arrivals for a particular cell form a Poisson point process.

Arrivals processes for different cells are independent.

The arrival rate is the same, say λ , for each cell.

When there is an arrival, the state of the cell instantaneously changes; the new state is computed based on the states of the cell and its neighbors just before the change (in the same manner as in the synchronous model). The new state may be equal to the old one.

The time of arrival and a random experiment may be involved in the computation.

A familiar example of a cellular system with the Poisson asynchrony is the Ising model [5] in the continuous time formulation of Glauber [6]. In this model a cell configuration is defined by the spin variables $s(c) = \pm 1$ specified at the cells c of a two or three dimensional array. When there is an arrival at a cell c , the spin $s(c)$ is changed to $-s(c)$ with probability p . With probability $1 - p$, the spin $s(c)$ remains unchanged. The probability p is determined using the values of $s(c)$ and neighbors $s(c')$ just before the update time.

It is instructive to review the computational procedures for Ising simulations. First,

the Ising simulationists realized that the standard procedure by Metropolis, Rosenbluth, Rosenbluth, Teller, and Teller [7] could be applied. In this procedure, the evolution of the configuration is simulated as a sequence of one-spin updates: Given a configuration, define the next configuration by choosing a cell c uniformly at random and changing or not changing the spin $s(c)$ to $-s(c)$ as required. In the original standard procedure time is discrete. Time continuity could have been simply introduced by letting the consecutive arrivals form the Poisson process with rate λN , where N is the total number of spins (cells) in the system.

The problem of long simulation runs became immediately apparent. Bortz, Kalos, and Lebowitz [8] developed a serial algorithm (the BKL algorithm) which avoids processing unsuccessful state change attempts, and reported up to a 10-fold speed-up over the straightforward implementation of the standard model. Ogielski [9] built special purpose hardware for speeding up the processing.

The BKL algorithm is serial. Attempts were made to speed up the Ising simulation by parallel computations (Friedberg and Cameron [10], Creutz [11]). However, in these computations the original Markov chain of the continuous time Ising model was modified to satisfy the computational procedure. The modifications do not affect the equilibrium behavior of the chain, and as such are acceptable if one studies only the equilibrium. In the cellular models however, the transient behavior is also of interest, and no model revision should be done.

This paper presents efficient methods for parallel simulation of the continuous time asynchronous cellular arrays without changing the model or type of asynchrony in favor of the computational procedure. The methods promise unlimited speed-up when the array and the parallel computer are sufficiently large. For the Poisson asynchrony case, it is also shown how the BKL algorithm can be incorporated, further contributing to speed-up.

For the Ising model, presented algorithms can be viewed as exact parallel counterparts to the standard algorithm by Metropolis et al. The latter has been known and believed to be inherently serial since 1953. Yet, the presented algorithms are parallel, efficient, and fairly simple. The “conceptual level” codes are rather short (see Figures 3.1, 3.2, 3.4, 3.6, and 3.7,). An implementation in a real programming language given in the Appendix is longer, of course, but still rather simple.

This paper is organized as follows: Section 2 presents a class of asynchronies and a comparison with other published proposals. Then Section 3 describes the new algorithms on the conceptual level. While the presented algorithms are simple, there is no simple theory which predicts speed-up of these algorithms for cellular arrays and parallel processors of large sizes. Section 4 contains a simplified computational procedure which predicts speed-ups faster than it takes to run an actual parallel program. The predictions made by this procedure are compared with actual runs and appear to be rather accurate. The procedure predicts speed-up of more than 8000 for the simulation of $10^5 \times 10^5$ Poisson asynchronous cellular array in parallel by 10^4 PEs. Actual speed-ups obtained thus far were: more than 16 on 25 PEs of the Balance (TM) computer and more than 1900 on 2^{14} PEs of the Connection Machine (R).

⁰Connection Machine is a registered trademark of Thinking Machines Corporation
Balance is a trademark of Sequent Computer Systems, Inc.

2. Model

Time t is continuous. Each cell c has a state $s = s(c)$. At random times, a cell is granted a chance to change the state. The changes, if they occur, are instantaneous events. Random attempts to change the state of a cell are independent of similar attempts for other cells.

The general model consists of two functions: *time_of_next_arrival* (\cdot) and *next_state* (\cdot). They are defined as follows: given the old state of the cell and the states of the neighbors just before time t , $s_{t-0}(\text{neighbors}(c))$, the next_state $s(c) = s_t(c)$ is

$$s_t(c) = \text{next_state}(c, s_{t-0}(\text{neighbors}(c)), \omega, t), \quad (1)$$

where the possibility $s_t(c) = s_{t-0}(c)$ is not excluded; and the time *next_t* of the next arrival is

$$\text{next_t} = \text{time_of_next_arrival}(c, s_{t-0}(\text{neighbors}(c)), \omega, t), \quad (2)$$

where always $\text{next_t} > t$.

In (1) and (2), ω denotes the result of a random experiment, e.g., coin tossing, $s(\text{neighbors}(c))$ denotes the indexed set of states of all the neighbors of c including c itself. Thus, if $\text{neighbors}(c) = \{c, c_1, c_2, c_3, c_4\}$, then $s(\text{neighbors}(c)) = (s(c), s(c_1), s(c_2), s(c_3), s(c_4))$. Subscript $t - 0$ expresses the idea of ‘just before t ’, e.g., $a_{t-0}(\tau) = \lim_{\tau \rightarrow t, \tau < t} a(\tau)$. According to (1), the value of $s(c)$ instantaneously changes at time t from $s_{t-0}(c)$ to $s_t(c)$. At time t , the value of $s(c)$ is already new. The ‘just before’ feature resolves a possible ambiguity if two neighbors attempt to change their states at the same simulated time.

Compare now the class of asynchronies defined by (2) with the ones proposed in the literature:

(A) Model 1 in [3] reads: “...the cells iterate randomly, one at a time.” Let p_c be the probability that cell c is chosen. Then the following choice of law (2) yields this model

$$\text{time_of_next_arrival}(c, \omega, t) = t - \frac{1}{p_c} \ln r(c, t, \omega),$$

where $r(c, t, \omega)$ is a random number uniformly distributed on $(0,1)$, and \ln is the natural logarithm, $\ln(x) = \log_e(x)$. For $p_{c_1} = p_{c_2} = \dots = \lambda$, the asynchrony was called the *Poisson asynchrony* in Section 1; it coincides with the one defined by the standard model [7], and by Glauber’s model [6] for the Ising spin simulations.

(B) Model 2 in [3] assigns “each cell a period according to a Gaussian distribution... The cells iterate one at a time each having its own definite period.” While it is not quite clear from [3] what is meant by a “definite period” (is it fixed for a cell over a simulation run?), the following choice of law (2) yields this model in a liberal interpretation:

$$\text{time_of_next_arrival}(c, \omega, t) = t + P_c^{-1}(r(\omega)),$$

where $P^{-1}(y) = x$ if $P(x) = y$, and $P_c(x)$ is the cumulative function for the Gaussian probability distribution with mean $m_c > 0$ and variance σ_c^2 . The probability of $\text{next_t} < t$ is small when $\sigma \ll m$ and is ignored in [3] if this interpretation is meant. In a less liberal interpretation, $\sigma_c \equiv 0$ for all c , and m_c is itself random and distributed according to the

Gaussian law. This case is even easier to represent in terms of model (2) than the previous one: $time_of_next_arrival(c, \omega, t) = t + m_c(\omega)$.

(3) Model (2) trivially extends to a synchronous simulation, where the initial state changes arrive at time 0 and then always $next_t - t$ is identical to 1. The first model in [4] is “to choose a number of cells at random and change only their values before continuing.” This is a variant of synchronous simulation; it is substantially different from both models (A) and (B) above. In (A) and (B), the probability is 1 that no two neighbors attempt to change their states at the same time. In contrast, in this model many neighboring cells are simultaneously changing their values. How the cells are chosen for update is not precisely specified in [4]. One way to choose the cells is to assign a probability weight p_c for cell c , $c = 1, 2, \dots, N$, and to attempt to update cell c at each iteration, with probability p_c , independent of any other decision. Such a method conforms with the law (2) because the method is local: a cell does not need to know what is happening at distant cells. The second model in [4] changes states of a fixed number A of randomly chosen cells at each iteration. If $A > 1$, this method is not local and does not conform with the law (2).

3. Algorithms

Elimination of ω . Deterministic computers represent randomness by using pseudo-random number generators. Thus, equations (1) and (2) are substituted in the computation by equations

$$s_t(c) = next_state(c, s_{t-0}(neighbors(c)), t), \quad (3)$$

and

$$next_t = time_of_next_arrival(c, s_{t-0}(neighbors(c)), t), \quad (4)$$

respectively, which do not contain the parameter of randomness ω .

This elimination of ω symbolizes an obvious but important difference between the simulated system and the simulator: In the simulated system, the observer, being a part of the system, does not know in advance the time of the next arrival. In contrast, the simulationist who is, of course, not a part of the simulated system, can know the time of the next arrival before the next arrival is processed.

For example, it is not known in advance when the next event from a Poisson stream arrives. However, in the simulation, the time $next_t$ of the next arrival is obtained in a deterministic manner, given the time t of the previous arrival:

$$next_t = t - \frac{1}{\lambda} \log_e(r(n(t))), \quad (5)$$

where λ is the rate, $r(n)$ is the n -th pseudo-random number in the sequence uniformly distributed on $(0, 1)$, and $n(t)$ is the invocation counter. Thus, after the previous arrival is processed, the time of the next arrival is already known. If needed, the entire sequence of arrivals can be precomputed and stored in a table for later use in the simulation, so that all future arrival times would be known in advance.

```

1. while  $t(c) < end\_time$ 
   {
2.   wait_until  $t(c) \leq \min_{c' \in neighbors(c)} t(c')$  ;
3.    $s(c) \leftarrow next\_state(c, s(neighbors(c)), t(c))$  ;
4.    $t(c) \leftarrow time\_of\_next\_arrival(c, s(neighbors(c)), t(c))$ 
   }

```

Figure 3.1: Asynchronous one-cell-per-one-PE algorithm

Asynchronous one-cell-per-one-PE algorithm. The algorithm in Figure 3.1 is the shortest of those presented in this paper.

To understand this code, imagine a parallel computer which consists of a number of PEs running concurrently. One PE is assigned to simulate one cell. The PE which is assigned to simulate cell c_0 , PE_{c_0} , executes the code in Figure 3.1 with $c = c_0$. The PEs are interconnected by the network which matches the topology of the cellular array. A PE can receive information from its neighbors. PE_c maintains state $s(c)$ and local simulated time $t(c)$. Variables $t(c)$ and $s(c)$ are visible (accessible for reading only) by the neighbors of c . Time $t(c)$ has no connection with the physical time in which the parallel computer runs the program except that $t(c)$ may not decrease when the physical time increases. At a given physical instance of simulation, different cells c may have different values of $t(c)$. Value end_time is a constant which is known to all PEs.

The algorithm in Figure 3.1 is very asynchronous: different PEs can execute different steps concurrently and can run at different speeds. A statement ‘wait_until *condition*’, like the one at Step 2 in Figure 3.1, does not imply that the *condition* must be detected immediately after it occurs. To detect the *condition* at Step 2 involving local times of neighbors a PE can poll its neighbors one at a time, in any order, with arbitrary delays, and without any respect to what these PEs are doing meanwhile.

Despite being seemingly almost chaotic, the algorithm in Figure 3.1 is free from deadlock. Moreover, it produces a unique simulated trajectory which is independent of executional timing, provided that:

- (i) for the same cell, the pseudo-random sequence is always the same,
- (ii) no two neighboring arrival times are equal.

Freedom from deadlock follows from the fact that the cell, whose local time is minimal over the entire array, is always able to make progress. (This guaranteed worst case performance, is substantially exceeded in an average case. See Section 4.)

The uniqueness of the trajectory can be seen as follows. By (ii), a cell c passes the test at Step 2 only if its local time $t(c)$ is smaller than the local time $t(c')$ of any its neighbor c' . If this is the case, then no neighbor c' is able to pass the test at Step 2 before c changes

its time at Step 4. This means that processing of the update by c is safe: no neighbor changes its state or time before c completes the processing. By (i), functions `next_state()` and `time_of_next_arrival()` are independent of the run. Therefore, in each program run, no matter what the neighbors of c are doing or trying to do, the next arrival time and state for c are always the same.

It is now clear why assumption (ii) is needed. If (ii) is violated by two cells c and c' which are neighbors, then the algorithm in Figure 3.1 does not exclude concurrent updating by c and c' . Such concurrent updating introduces an indeterminism and inconsistency. A scenario of the inconsistency can be as follows: at Step 3 the *old* value of $s(c')$ is used to update state $s(c)$, but immediately following Step 4 uses the *new* value of $s(c')$ to update time $t(c)$.

In practice, the algorithm in Figure 3.1 is safe, when $next_t(c) - t(c)$ for different c are independent random samples from a distribution with a continuous density, like an exponential distribution. In this case, (ii) holds with probability 1. Unless the pseudo-random number generators are faulty, one may imagine only one reason for violating (ii): finite precision of computer representation of real numbers.

Synchronous one-cell-per-one-PE algorithm. If (ii) can be violated with a positive probability (if t takes on only integer values, for example), then the errors might not be tolerable. In this case the synchronous algorithm in Figure 3.2 should be used.

Observe that while the algorithm in Figure 3.2 is synchronous, it is able to simulate correctly both synchronous and asynchronous systems. Two main additions in the algorithm in Figure 3.2 are: private variables `new_s` and `new_t` for temporal storage of updated s and t , and synchronization barriers ‘synchronize’. When a PE hits a ‘synchronize’ statement it must wait until all the other PEs hit a ‘synchronize’ statement; then it may resume. Two dummy synchronizations at Steps 9 and 10 are executed by idling PEs in order to match synchronizations at Steps 5 and 8 executed by non-idling PEs.

When (ii) is violated, the synchronous algorithm avoids the ambiguity and indeterminism (which in this case are possible in the asynchronous algorithm) as follows: in processing concurrent updates of two neighbors c and c' for the same simulated time $t = t(c) = t(c')$, first, c and c' read states s_{t-0} and times t of each other and compute their private `new_s`'s and `new_t` (Steps 3 and 4 in Figure 3.2); then, after the synchronization barrier at Step 5, c and c' write their states and times at Steps 6 and 7, thus making sure that no write interferes with a read.

Aggregation. In the two algorithms presented above, one PE hosts only one cell. Such an arrangement may be wasteful if the communication between PEs dominates the computation internal to a PE. A more efficient arrangement is to assign several cells to one PE. For concreteness, consider a two-dimensional $n \times n$ array with periodic boundary conditions. Let n be a multiple of m and $(n/m)^2$ PEs be available. PEC carries $m \times m$ subarray C , where $C = 1, 2, \dots, (n/m)^2$. (Capital C will be used without confusion to represent both the subarray index and the set of cells c the subarray comprises, e.g. as in $c \in C$) A fragment of a square cellular array in an example of such an aggregation is

```

1. while  $t(c) < end\_time$ 
   {
2.   if  $t(c) \leq \min_{c' \in neighbors(c)} t(c')$  then
     {
3.        $new\_s \leftarrow next\_state(s(neighbors(c)), t(c))$ ;
4.        $new\_t \leftarrow time\_of\_next\_arrival(c, t(c))$ ;
5.       synchronize;                               /* barrier 1 */
6.        $s(c) \leftarrow new\_s$ ;
7.        $t(c) \leftarrow new\_t$ ;
8.       synchronize                               /* barrier 2 */
     }
   else {
9.       synchronize;                               /* barrier 1 */
10.      synchronize                               /* barrier 2 */
     }
   }

```

Figure 3.2: Synchronous one-cell-per-one-PE algorithm

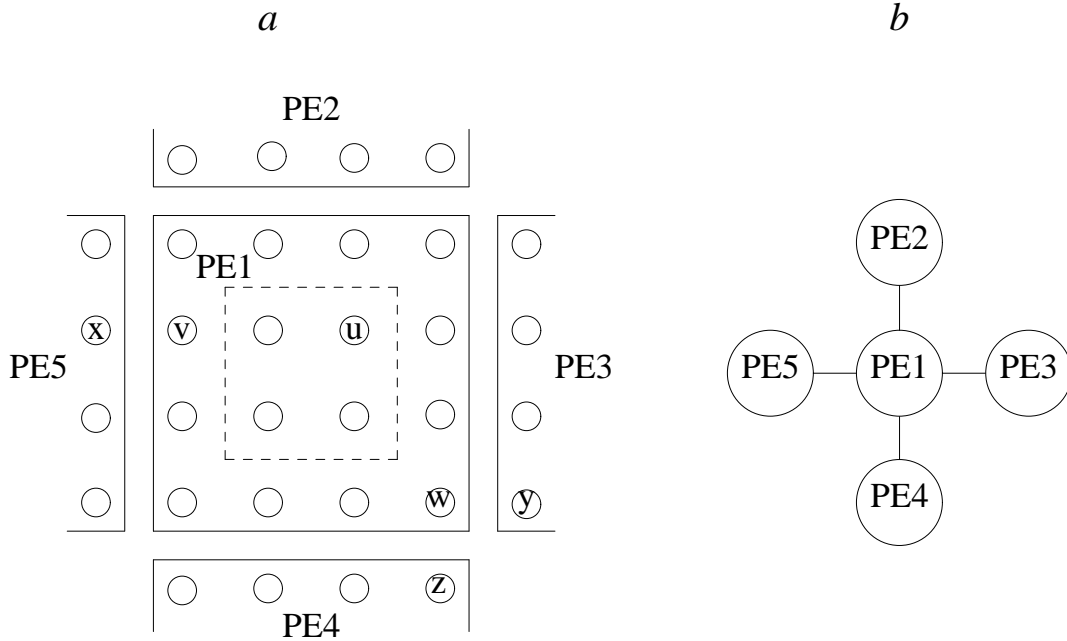


Figure 3.3: Aggregation: *a*) mapping of cells to PEs, *b*) the interconnection among the PEs which supports the neighborhood topology among the cells

represented in Figure 3.3a, wherein $m = 4$.

The neighbors of a cell carried by PE1 are cells carried by PE2, PE3, PE4, or PE5. PE1 has direct connections with these four PEs (Figure 3.3b). Given cell c in the subarray hosted by PE1, one can determine with which neighboring PEs communication is required in order to learn the states of the neighboring cells. Let $W(c)$ be the set of these PEs. Examples in Figure 3.3a : $W(u)$ is empty, $W(v) = \{\text{PE5}\}$, $W(w) = \{\text{PE3}, \text{PE4}\}$.

Figure 3.4 presents an aggregated variant of the algorithm in Figure 3.1. PEC , which hosts subarray C , maintains the local time register $T(C)$. PEC_0 simulates the evolution of its subarray using the algorithm in Figure 3.4 with $C = C_0$. Each cell $c \in C$ is represented in the memory of PEC by its current state $s(c)$ and its next arrival time $t(c)$. Note that unlike the one-cell-per-one-PE algorithm, the $t(c)$ does not represent the current local time for cell c . Instead, local times of all cells within subarray C are the same, $T(C)$.

$T(C)$ moves from one $t(c)$ to another in the order of increasing value. Three successive iterations of this algorithm are shown in Figure 3.5, where the subarray C consists of four cells: $C = \{1, 2, 3, 4\}$. Circles in Figure 3.5 represent arrival points in the simulated time. A crossed-out circle represents an arrival which has just been processed, i.e., Steps 3, 4, and 5 of Figure 3.4 have just been executed, so that $T(C)$ has just taken on the value of the processed old arrival time $t(c)$, while the $t(c)$ has taken on a new larger value. This new value is pointed to by an arrow from $T(C)$ in Figure 3.5. It is obvious that always $t(c) \geq T(C)$ if $c \in C$.

Local times $T(C)$ maintained by different PEC might be different. A wait at Step 3

```

1. while  $T(C) < end\_time$ 
   {
2.   select a cell  $c$  in the subarray  $C$  such that
       $t(c) = \min_{c' \in C} t(c')$  and assign  $T(C) \leftarrow t(c)$ ;
3.   wait_until  $T(C) \leq \min_{c' \in W(c)} T(C')$  ;
4.    $s(c) \leftarrow next\_state(c, s(neighbors(c)), t(c))$  ;
5.    $t(c) \leftarrow time\_of\_next\_arrival(c, s(neighbors(c)), t(c))$ 
   }

```

Figure 3.4: Asynchronous many-cells-per-one-PE algorithm. General asynchrony

cannot deadlock the execution since the PEC whose $T(C)$ is the minimum over the entire cellular array is always able to make a progress.

Assuming property (ii) as above, the algorithm correctly simulates the history of updates. The following example may serve as an informal proof of this statement. Suppose PE1 is currently updating the state of cell v (see Figure 3.3a) and its local time is T_1 . Since $W(v) = \{PE5\}$, this update is possible because the local time of PE5, T_5 , is currently larger than T_1 . At present, PE1 receives the state of x from PE5 in order to perform the update. This state is in time T_5 , i.e., in the future with respect to local time T_1 . However, the update is correct, since the state of x was the same at time T_1 , as it is at time T_5 .

Indeed, suppose the state of x were to be changed at simulated local time T , $T_1 < T < T_5$. At the moment when this change would have been processed by PE5, the local time of PE1 would have been larger than T , and T would have been the local time of PE5. After this processing has supposedly taken place, the local time of PE1 should not decrease. Yet at the present it is T_1 , which is smaller than T . This contradiction proves that the state of x cannot in fact change in the interval (T_1, T_5) .

In the example in Figure 3.5, only one $t(c)$ supplies $\min_{c' \in C} t(c')$. However, the algorithm in Figure 3.4 at Step 2 commands to select *a* cell not *the* cell. This covers the unlikely situation of several cells having the same minimum time. If $next_t(c) - t(c)$ for different c are independent random samples from a distribution with a continuous density, this case occurs with the probability zero. On the other hand, if several cells can, with positive probability, update simultaneously, a synchronous version of the aggregated algorithm should be used instead. To eliminate indeterminism and inconsistency, the latter would use synchronization and intermediate storage techniques. These techniques were demonstrated in the algorithm in Figure 3.2 and their discussion is not repeated here.

For an important special case of **Poisson asynchrony in the aggregated algorithm**, the algorithm of Figure 3.4 is rewritten in Figure 3.6. This specialization capitalizes on the additive property of Poisson streams, specifically, on the fact that sum of k independent Poisson streams with rate λ each is a Poisson stream with rate λk . In the algorithm, $k = number_of_cells_in_C$; this k is equal to m^2 in the special case of partitioning into $m \times m$

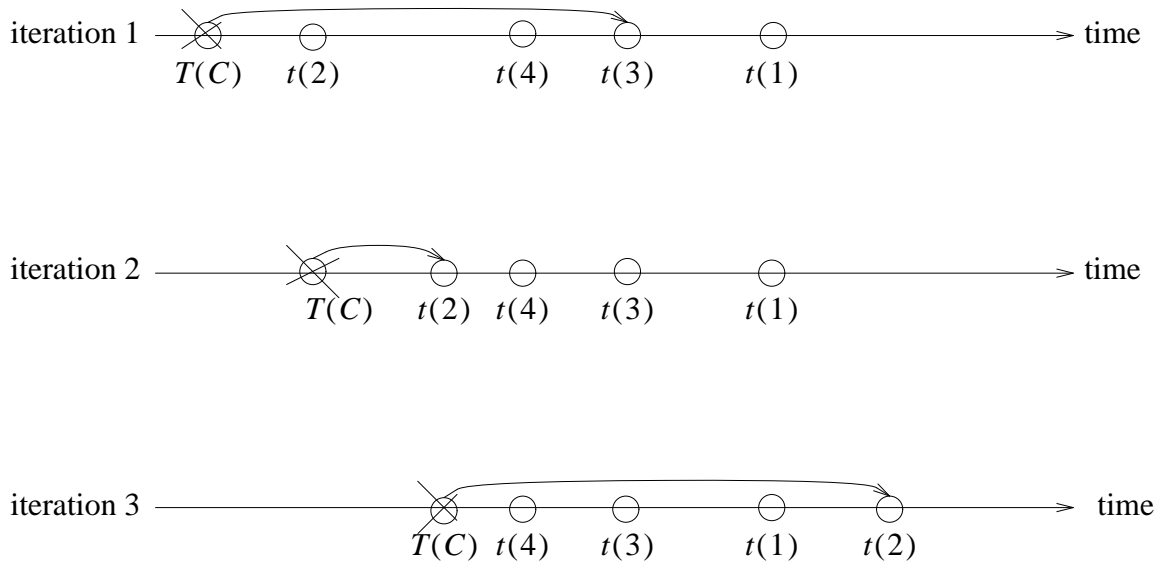


Figure 3.5: $T(C)$ slides along a sequence of $t(c)$'s in successive iterations of the aggregated algorithm

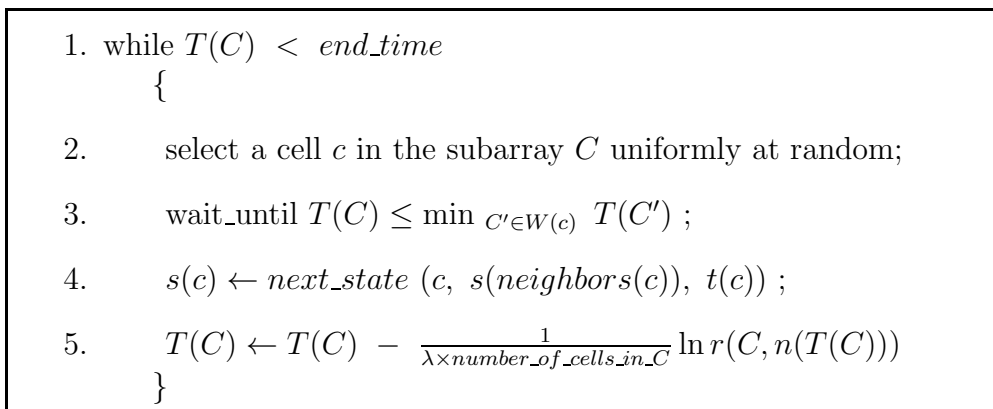


Figure 3.6: Asynchronous many-cells-per-one-PE algorithm. Poisson asynchrony

subarrays. Unlike the general algorithm of Figure 3.4, in the specialization in Figure 3.6 neither individual streams for different cells are maintained, nor future arrivals $t(c)$ for cells are individually computed. Instead, a single cumulative stream is simulated and cells are delegated randomly to meet these arrivals.

At Step 5 in Figure 3.6, $r(C, n(T(C)))$ is an $n(T(C))$ -th pseudo-random number in the sequence uniformly distributed in $(0,1)$. It follows from the notation that each PE has its own sequence. If this sequence is independent of the run (which is condition (i) above) and if updates for neighboring cells never coincide in time (which is condition (ii) above), then this algorithm produces a unique reproducible trajectory. The same statement is also true for the algorithm in Figure 3.4. However, uniqueness provided by the algorithm in Figure 3.6 is weaker than the one provided by the algorithm in Figure 3.4: if the same array is partitioned differently and/or executed with different number of PEs, a trajectory produced by the algorithm in Figure 3.6 may change; however, a trajectory produced by the algorithm in Figure 3.4 is invariant for such changes given that each cell c uses its own fixed pseudo-random sequence.

Efficiency of aggregated algorithms. Both many-cells-per-one-PE algorithms in Figure 3.4 and Figure 3.6 are more efficient than the one-cell-per-one-PE counterparts in Figure 3.1 and Figure 3.2. This additional efficiency can be explained in the example of the square array, as follows: In the algorithms in Figure 3.1 and Figure 3.2, a PE may wait for its four neighbors. However, in the algorithms in Figure 3.4 and Figure 3.6, a PE waits for at most two neighbors. For example, when the state of cell w in Figure 3.3a is updated, PE1 might wait for PE3 and PE4. Moreover, for at least $(m - 2)^2$ cells c out of m^2 , PE1 does not wait at all, because $W(c) = \emptyset$. The cells c such that $W(c) = \emptyset$ form the dashed square in Figure 3.3a.

This additional efficiency becomes especially large if, instead of set $neighbors(c)$ in the original formulation of the model, one uses sets

$$neighbors^2(c) \stackrel{\text{def}}{=} next_to_nearest_neighbors(c) \tag{6}$$

or, more generally, q -th degree neighborhood, $neighbors^q(c)$. The latter is defined for $q > 1$ inductively

$$neighbors^q(c) \stackrel{\text{def}}{=} neighbors(neighbors^{q-1}(c)) \tag{7}$$

where $neighbors(S)$ for a set S of cells is defined as $neighbors(S) \stackrel{\text{def}}{=} \bigcup_{c \in S} neighbors(c)$.

It is easy to rewrite the algorithms in Figure 3.1 and Figure 3.2 for the case $q > 1$. The obtained codes have low efficiency however. For example, in the square array case, one has $|neighbors^q(c)| - 1 = 2q(q + 1)$. Thus, if $q = 2$, a cell might have to wait for 12 cells in order to update. In the same example, if one PE carries an $m \times m$ subarray, and $m > q$, then the PE waits for at most three other PEs no matter how large the q is. Moreover, if $m > 2q$ then in $(m - 2q)^2$ cases out of m^2 the PE does not wait at all.

The BKL algorithm [8] was originally proposed for Ising spin simulations. It was noticed that the probability p to flip $s(c)$ takes on only a finite (and small) number d of

values p_1, \dots, p_d , each corresponding to one or several combinations of old values of $s(c)$ and neighboring spins $s(c')$. Thus the algorithm splits the cells into d pairwise disjoint classes $\Gamma_1, \Gamma_2, \dots, \Gamma_d$. The rates λp_k of changes (not just of the attempts to change) for all $c \in \Gamma_k$ are the same. At each iteration, the BKL algorithm does the following:

- (a) Selects Γ_{k_0} at random according to the weights $|\Gamma_k|p_k$, $k = 1, 2, \dots, d$, and selects a cell $c \in \Gamma_{k_0}$ uniformly at random.
- (b) Flips the state of the selected cell, $s(c) \leftarrow -s(c)$.
- (c) Increases the time by $-\log_e(r)/(\lambda(\sum_{1 \leq k \leq d} |\Gamma_k|p_k))$, where r is a pseudo-random number uniformly distributed in $(0,1)$.
- (d) Updates the membership in the classes.

If the asynchrony law is Poisson, the idea of the BKL algorithm can be applied also to a deterministic update. Here the probability p of change takes on just two values:

$p_1 = 0$ if $next_s(c) = s(c)$, and $p_2 = 1$ if $next_s(c) \neq s(c)$.

Accordingly, there are two classes: Γ_0 , the cells which are not going to change and Γ_1 , the cells which are going to change. As with the original BKL algorithm, a substantial overhead is required for maintaining an account of the membership in the classes (Step (d)). The BKL algorithm is justified only if a large number of cells are not going to change their states. The latter is often the case. For example, in the Conways's synchronous *Game of Life* (Gardner [12]) large regions of white cells ($s(c) = 0$) remain unchanged for many iterations with very few black cells ($s(c) = 1$). One would expect similar behavior for an asynchronous version of the Game of Life.

The basic BKL algorithm is serial. To use it on a parallel computer, an obvious idea is to run a copy of the serial BKL algorithm in each subarray carried by a PE. Such a procedure, however, causes roll-backs, as seen in the following example:

Suppose PE1 is currently updating the state of cell v (Figure 3.3a) and its local time is T_1 , while the local time of PE5, T_5 , is larger than T_1 . Since x is a nearest neighbor to B , x 's membership might change because of v 's changed state. Suppose x 's membership were to indeed change. Although this change would have been in effect since time T_1 , PE5, which is responsible for x , would learn about the change only at time $T_5 > T_1$. As the past of PE5 is not, therefore, what PE5 has believed it to be, interval $[T_1, T_5]$ must have been simulated by PE5 incorrectly, and must be played again. This original roll-back might cause a cascade of secondary roll-backs, third generation roll-backs etc.

A modified BKL algorithm applies the original BKL procedure only to a subset of the cells, whereas the procedure of the standard model is applied to the remaining cells. More specifically: An additional separate class Γ_0 is defined. Unlike other Γ_k , $k > 0$, class Γ_0 always contains the same cells. Steps (a) - (d) are performed as above with the following modifications:

- 1) The weight of Γ_0 at step (a) is taken to be $|\Gamma_0|$.
- 2) If the selected c belongs to Γ_0 , then at step (b) the state of c may or may not change. The probability p of change is determined as in the standard model.
- 3) The time at step (c) should be increased by $-\log_e(r)/(\lambda(|\Gamma_0| + \sum_{1 \leq k \leq d} |\Gamma_k| p_k))$, where $r = r(c, n(t))$ is a pseudo-random number uniformly distributed in $(0, 1)$.

Now consider again the subarray carried by PE1 in Figure 3.3a. The subarray can be subdivided into the $(m - 2) \times (m - 2)$ “kernel” square and the remaining boundary layer. If first degree neighborhood, $neighbors(c)$, is replaced with the q -th degree neighborhood, $neighbors^q(c)$, then the kernel is the central $(m - 2q) \times (m - 2q)$ square, and the boundary layer has width q . In Figure 3.3a, the cells in the dashed square constitute the kernel with $q = 1$. To apply the modified BKL procedure to the subarray carried by PE1, the boundary layer is declared to be the special fixed class Γ_0 . Similar identification is done in the other subarrays. As a result, the fast concurrent BKL procedures on the kernels are shielded from each other by slower procedures on the layers.

The roll-back is avoided, since state change of a cell in a subarray does not constitute state or membership change of a cell in another subarray. Unless the performance of PE1 is taken into account, the neighbors of PE1 can not even tell whether PE1 uses the standard or the BKL algorithm to update its kernel. As the size of the subarray increases, so does both the relative weight of the kernel and the fraction of the fast BKL processing.

Generating the output. Consider the task of generating cellular patterns for specified simulated times. A method for performing this task in a serial simulation or a parallel simulation of a synchronous cellular array is obvious: as the global time reaches a specified value, the computer outputs the states of all cells. In an asynchronous simulation, the task becomes more complicated because there is no global time: different PEs may have different local times at each physical instance of simulation.

Suppose for example, one wants to see the cellular patterns at regular time intervals $K_0\Delta t$, $(K_0+1)\Delta t$, $(K_0+2)\Delta t$, ... on a screen of a monitor attached to the computer. Without getting too involved in the details of performing I/O operations and the architecture of the parallel computer, it would be enough to assume that a separate process or processes are associated with the output; these processes scan an output buffer memory space allocated in one or several PEs or in the shared memory; the buffer space consists of B frames, numbered $0, 1, \dots, B - 1$, each capable of storing a complete image of the cellular array for one time instance. The output processes draw the image for time $K\Delta t$ on the screen as soon as the frame number $rem(K/B)$ (the remainder of the integer division K by B) is full and the previous images have been shown. Then the frame is flashed for the next round when it will be filled with the image for time $(K + B)\Delta t$ and so on.

The algorithm must fill the appropriate frame with the appropriate data as soon as both data and the frame become available. The modifications that enable the asynchronous al-

```

/* Initially  $K = K_0, T(C) < K_0\Delta t$  */

1. while  $T(C) < end\_time$ 
   {
2.   select a cell  $c$  in the subarray  $C$  such that
       $t(c) = \min_{c' \in C} t(c')$  and assign  $new\_T \leftarrow t(c)$ ;
3.   while  $new\_T > K\Delta t$ 
      {
4.     wait_until frame  $rem(K/B)$  is available;
5.     store image  $s(C)$  into frame  $rem(K/B)$ ;
6.      $K \leftarrow K + 1$ 
       };
7.    $T(C) \leftarrow new\_T$ ;
8.   wait_until  $T(C) \leq \min_{c' \in W(c)} T(C')$  ;
9.    $s(c) \leftarrow next\_state(c, s(neighbors(c)), t(c))$  ;
10.   $t(c) \leftarrow time\_of\_next\_arrival(c, s(neighbors(c)), t(c))$ 
     }

```

Figure 3.7: Generating the output in the aggregated asynchronous algorithm

gorithm in Figure 3.4 to perform this task are presented in Figure 3.7. In this algorithm, variables new_T and K are private (i.e., local to PE) and Δt and K_0 are constants whose values are the same for all the PEs. Note that different PEs may fill different frames concurrently. If the slowest PE is presently filling an image for time $K\Delta t$, then the fastest PE is allowed to fill the image for time no later than $(K + B - 1)\Delta t$. An attempt by the fastest PE to fill the image for time $(K + B)\Delta t$ will be blocked at Step 4, until the frame number $rem(K/B) = rem((K + B)/B)$ becomes available.

Thus, the finiteness of the output buffer introduces a restriction which is not present in the original algorithm in Figure 3.4. According to this restriction, the lag between concurrently processed local times cannot exceed a certain constant. The exact value of the constant in each particular instance depends on the relative positions of the update times within the Δt -slots. In any case, the constant is not smaller than $(B - 1)\Delta t$ and not larger than $B\Delta t$.

However, even with a single output buffer segment, $B = 1$, the simulation does not become time-driven. In this case, the concurrently processed local times might be within a distance of up to Δt of each other, whereas Δt might be relatively large. No precision of update time representation is lost, although efficiency might degrade when both Δt and B become too small, see Section 4.

4. Performance assessment: experiments and simulations

Modeling and analysis of asynchronous algorithms is a difficult theoretical problem. Strictly speaking, the following discussion is applicable only to synchronous algorithms. However, one may argue informally that the performance of an asynchronous algorithm is not worse than that of its synchronous counterpart, since expensive synchronizations are eliminated.

First, consider the synchronous algorithm in Figure 3.2. Let N be the size of the array and N_0 be the number of cells which passed the test at Step 2, Figure 3.2. The ratio of useful work performed, to the total work expended at the iteration is N_0/N . This ratio yields the *efficiency* (or *utilization*) at the given iteration. Assuming that in the serial algorithm all the work is useful, and that the algorithm performs the same computation as its parallel counterpart, the speed-up of the parallel computation is the average efficiency times the number of PEs involved. Here the averaging is done with equal weights over all the iterations.

In the general algorithms, $next_t(c)$ is determined using the states of the neighbors of c . However, in the important applications, such as an Ising model, $next_t(c)$ is independent of states. The following assessment is valid only for this special case of independence. Here the configuration is irrelevant and whether the test succeeds or not can be determined knowing only the times at each iteration. This leads to a simplified model in which only local times are taken into account: at an iteration, the local time of a cell is incremented if the time does not exceed the minimum of the local times of its neighbors.

A simple (serial) algorithm which updates only local times of cells $t(c)$ according to the rules formulated above was exercised for different array sizes n and three different dimensions: for an n -element circular array, an $n \times n$ toroidal array, and for $n \times n \times n$ array with periodic boundary conditions. Two types of asynchronies are tried: the Poisson asynchrony for

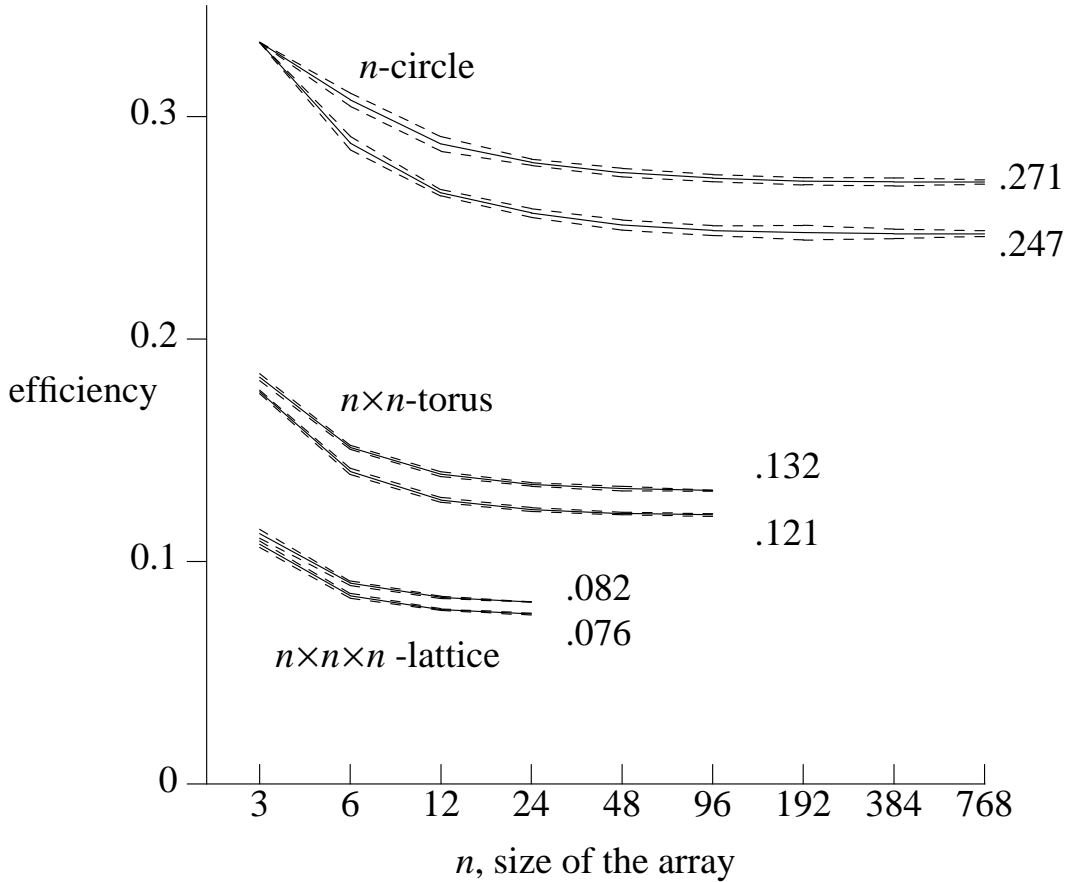


Figure 4.1: Performance of the Ising model simulation. One-cell-per-one-PE case

which $next_t - t$ is distributed exponentially, and the asynchrony for which $next_t - t$ is uniformly distributed in $(0,1)$. In both cases, random time increments for different cells are independent.

The results of these six experiments are given in Figure 4.1. Each solid line in Figure 4.1 is enclosed between two dashed lines. The latter represent 99.99% Student's confidence intervals constructed using several simulation runs, that are parametrically the same but fed with different pseudo-random sequences. In Figure 4.1, for each array topology there are two solids lines. The Poisson asynchrony always corresponds to the lower line. The corresponding limiting values of performances (when n is large) are also shown near the right end of each curve. For example, the efficiency in the simulation of a large $n \times n$ array with the Poisson asynchrony is about 0.121, with the other asynchrony, it is about 0.132.

No analytical theory is available for predicting these values or even proving their separation from zero when $n \rightarrow +\infty$. It follows from Figure 4.1 that replacing exponential distribution of $next_t - t$ with the uniform distribution results in efficiency increase from 0.247 to 0.271 for a large n -circle ($n \rightarrow +\infty$). The efficiency can be raised even more. If $next_t - t = r^{1/8}$, where r is distributed uniformly in $(0,1)$, then in the limit $n \rightarrow +\infty$, with

the Student's confidence 99.99%, the efficiency is 0.3388 ± 0.0012 . It is not known how high the efficiency can be raised this way (degenerated cases, like a synchronous one, in which the efficiency is 1, are not counted).

An efficiency of 0.12 means the speed-up of $0.12 \times N$; for $N = 2^{14}$ this comes to more than 1900. This assessment is confirmed in an actual full scale simulation experiment performed on $2^{14} = 128 \times 128$ PEs of a Connection Machine (R) (a quarter of the full computer). This SIMD computer appears well-suited for the synchronous execution of the one-cell-per-one-PE algorithm in Figure 3.2 on a toroidal array, Poisson asynchrony law. Since an individual PE is rather slow, it executes several thousand instructions per second, and its absolute speed is not very impressive: It took roughly 1 sec. of real time to update all 128×128 spins when the traffic generated by other tasks running on the computer was small (more precise measurement was not available). This includes about $8.3 \approx (0.12)^{-1}$ rounds of the algorithm, several hundred instructions of one PE per round.

The 12% efficiency in the one-cell-per-one-PE experiments could be greatly increased by aggregation. The many-cells-per-one-PE algorithm in Figure 3.6 is implemented as a C language parallel program for a Balance (TM) computer, which is a shared memory MIMD bus machine. The $n \times n$ array was split into $m \times m$ subarrays, as shown in Figure 3.3, where n is a multiple of m . Because the computer has 30 PEs, the experiments could be performed only with $(n/m)^2 = 1, 4, 9, 16,$ and 25 PEs for different n and m .

Along with these experiments, a simplified model, similar to the one-cell-per-one-PE case, was run on a serial computer. In this model, quantity $h(C) \stackrel{\text{def}}{=} \lambda T(C)$ is maintained for each PE, $C = 1, \dots, (n/m)^2$. The update of $h(C)$ is arranged in rounds, wherein each $h(C)$ is updated as follows:

(i) with probability $p_0 = (m - 2)^2/m^2$, PEC updates $h(C)$:

$$h(C) \leftarrow h(C) - \ln^r(C, n(h(C))), \quad (8)$$

where r and \ln are the same as in Step 5 in Figure 3.6. Here p_0 is the probability that the PE chooses a cell c so that $|W(c)| = 0$;

(ii) with probability $p_1 = 4(m - 2)/m^2$, the PE must check the $h(C')$ of one of its four neighbors C' before making the update. The C' is chosen uniformly at random among the four possibilities. If $h(C') \geq h(C)$, then $h(C)$ gets an increment according to (8); otherwise, $h(C)$ is not updated. Here p_1 is the probability that PE will choose a cell c in an edge but not in a corner, so that $|W(c)| = 1$

(iii) with the remaining probability $p_2 = 4/m^2$, the PE checks $h(C')$ and $h(C'')$ of two of its adjacent neighbors (for example in Figure 3.3, neighbors PE2 and PE3 can be involved in the computation for PE1). The two neighbors are chosen uniformly at random from the four possibilities. Again, if both $h(C') \geq h(C)$ and $h(C'') \geq h(C)$, then $h(C)$ gets an increment according to (8); otherwise, $h(C)$ is not updated. Here p_2 is the probability to choose a cell c in a corner, so that $|W(c)| = 2$.

As in the previous case, this simplified model simulates a possible but not obligatory synchronous timing arrangement for executing the real asynchronous algorithm. Figure 4.2 shows excellent agreement between actual and predicted performances for the aggregated

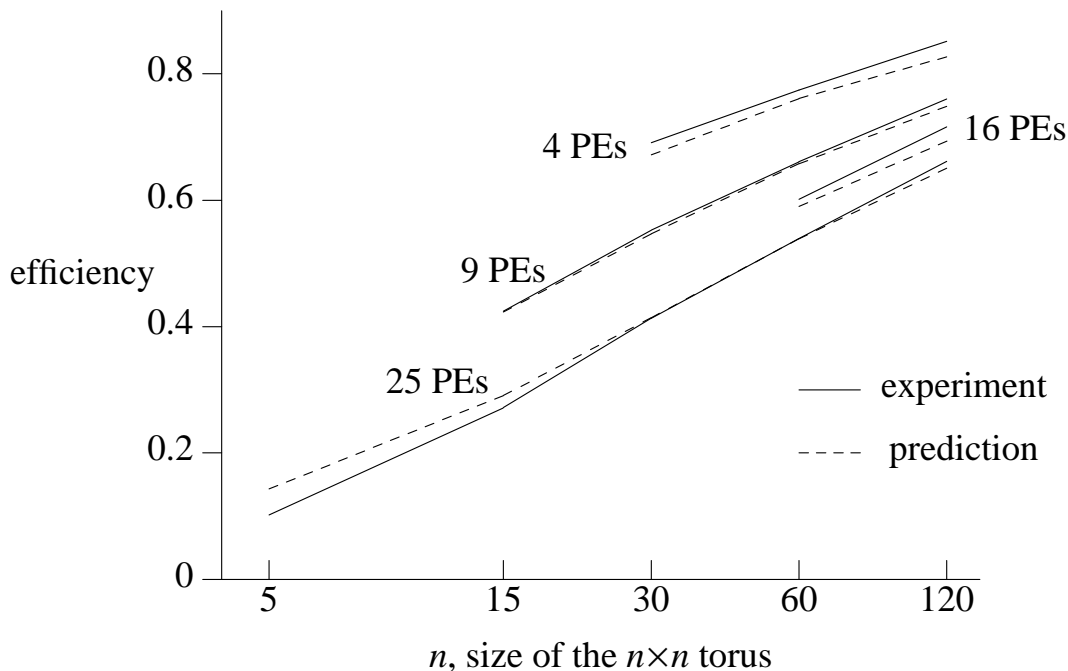


Figure 4.2: Performance of the Ising model simulation. Many-cells-per-one-PE case

Ising model. The efficiency presented in Figure 4.2 is computed as

$$\text{efficiency} = \frac{\text{serial execution time}}{\text{number of PEs} \times \text{parallel execution time}} \quad (9)$$

The parallel speed-up can be found as efficiency \times number of PEs. For 25 PEs simulating a 120×120 Ising model, efficiency is 0.66; hence, the speed-up is greater than 16. For the currently unavailable sizes, when 10^4 PEs simulate a $10^4 \times 10^4$ array, the simplified model predicts an efficiency of about 0.8 and a speed-up of about 8000.

In the experiments reported above, the lag between the local times of any two PEs was not restricted. As discussed in Section 3, an upper bound on the lag might result from the necessity to produce the output. To see how the bound affects the efficiency, one experiment reported in Figure 4.2, is repeated with various finite values of the lag bound. In this experiment, an $n \times n$ array is simulated and one PE carries an $m \times m$ subarray, where $n = 384$ and $m = 12$. The results are presented in Figure 4.3.

In Figure 4.3, the unit of measure for a lag is the expectation of time intervals between consecutive arrivals for a cell. For lag bounds greater than 16, degradation of efficiency is almost unnoticeable, when compared with the base experiment where lag = ∞ . Substantial degradation starts at about 8; for the unity lag bound, the efficiency is about half that of the base experiment. However, even for lag bound 0.3, the simulation remains practical, with an efficiency of about 0.1; since 1024 PEs execute the task, this efficiency means a speed-up of more than 100.

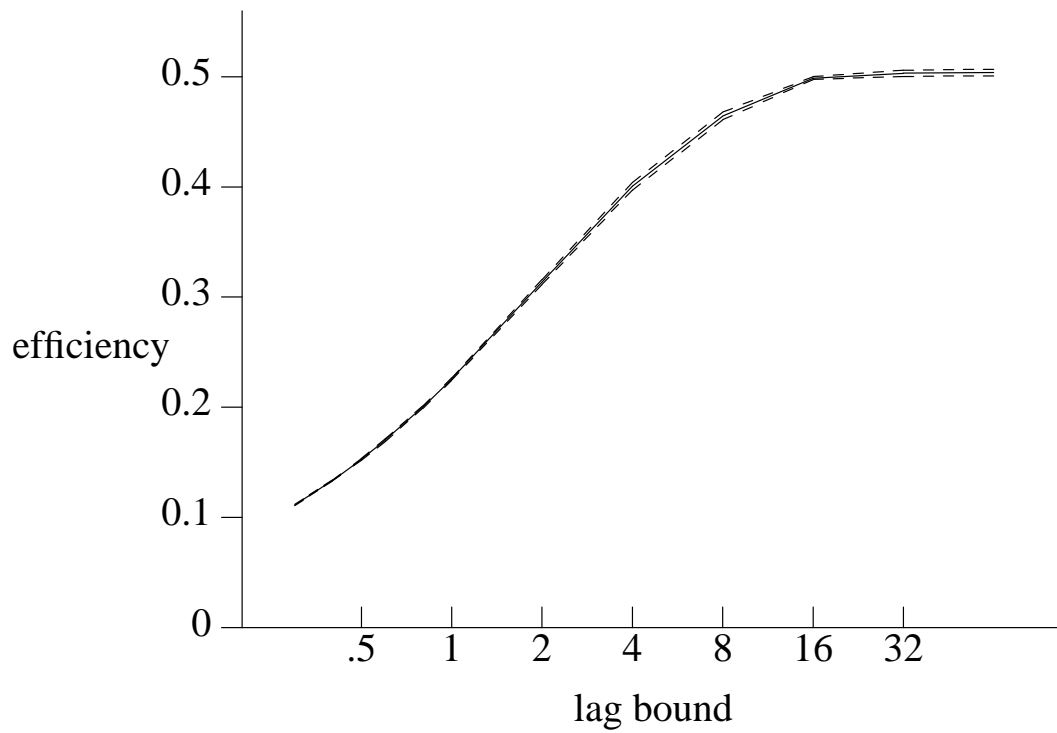


Figure 4.3: Efficiency degradation caused by bounded lag

5. Conclusion

This paper demonstrates an efficient parallel method for simulating asynchronous cellular arrays. The algorithms are quite simple and easily implementable on appropriate hardware. In particular, each algorithm presented in the paper can be implemented on a general purpose asynchronous parallel computer, such as the currently available bus machines with shared memory. The speed of such implementation depends on the speed of PEs and the efficiency of the communication system. A crucial condition for success in such implementation is the availability of a good parallel generator of pseudo-random numbers. To assure reproducibility, each PE should have its own reproducible pseudo-random sequence.

The proposed algorithms present a number of challenging mathematical problems, for example, the problem of proving that efficiency tends to a positive limit when the number of PEs increases to infinity.

Acknowledgments.

I acknowledge the personnel of the Thinking Machine Corp. for their kind invitation, and help in debugging and running the parallel *LISP program on one of their computers. Particularly, the help of Mr. Gary Rancourt and Mr. Bernie Murray was invaluable. Also, I thank Andrew T. Ogielski and Malvin H. Kalos for stimulating discussions, Debasis Mitra for a helpful explanation of a topic in Markov chains, and Brigid Moynahan for carefully reading the text.

References

- [1] S. Geman and D. Geman, Stochastic relaxation, Gibbs distributions, and the Bayesian restoration of images, *IEEE Transactions on pattern analysis and machine intelligence*, **PAMI-6**, 6, (Novem. 1984), 721–741.
- [2] B. D. Lubachevsky and D. Mitra, A chaotic asynchronous algorithm for computing the fixed point of a nonnegative matrix of unit spectral radius, *Journal of the ACM*, **33**, 1 (1986), 130–150.
- [3] T. E. Ingerson and R. L. Buvel, Structure in asynchronous cellular automata, *Physica*, **10D** (1984), 59–68.
- [4] M. I. Hoffman, A cellular Automation Model Based on Cortical Physiology, *Complex Systems*, **1**, (1987), 187–202.
- [5] F. Ising, Beitrag zur theorie des ferromagnetismus, *Z. Physik*, **31** (1925), 253–258.
- [6] R. J. Glauber, Time-dependent statistics of the Ising model, *Journ. Math. Physics*, **4**, no.2 (1963), 294–307.
- [7] N. Metropolis, A.W. Rosenbluth, M.N. Rosenbluth, A.H. Teller, and E. Teller, Equation of state calculations by fast computing machines, *Journ. Chem. Physics*, **21**, no.6 (1953), 1087–1092.
- [8] A. B. Bortz, M. H. Kalos, and J. T. Lebowitz, A new algorithm for Monte Carlo simulation of Ising spin systems, *J. Comp. Physics*, **17** (1975), 10–18.
- [9] A. T. Ogielski, Dynamics of three-dimensional Ising spin glasses in thermal equilibrium, *Physical Review B*, **32**, no.11 (1985), 7384–7398.
- [10] R. Friedberg, and J. E. Cameron, Test of the Monte Carlo method: fast simulation of a small Ising lattice, *Journ. Chem. Physics*, **52**, no.12 (1970), 6049–6058.
- [11] M. Creutz, Deterministic Ising dynamics, *Ann. Phys.* **167**, no. 62 (1986), pp. 62–72.
- [12] M. Gardner, Mathematical games. The fantastic combinations of John Conway’s new_solitaire game “life”, *Scientific American*, October 1970, 120–124.

APPENDIX: a working code of Ising simulation

C language program for the BALANCE parallel computer; the code is used for timing only and contains no i/o; the code of the pseudo-random number generator is not included

```
#include <pp.h>
#include <math.h>
#include <sys/tmpctl.h>

#define SHARED_MEM_SIZE (sizeof(double)*10000)
#define END_TIME 1000.
#define A 24          /* side of small square a PE takes care of*/
#define M 5          /* number of PEs along a side of the big square*/

shared int nPEs = M*M, spin[M*A][M*A];
shared float time[M][M]; /*local times on subarrays*/
shared float prob[10]; /* probabilities of state change */
shared float J = 1., H = 0.; /* Energy= -J sum spin spin' - H sum spin */
shared float T = 1.; /* Temperature */
shared int ato2 = A*A;
shared int am = A*M;

main()
{
    int i,j,child_id, my_spin, sum_nei, index, bit;
    float d_E, x;
    double frand();

    /* compute flip probabilities */
    for (i = 0; i < 5 ; i++)
        for (j = 0; j < 2; j++)
            {index = i + 5*j; /* index = 0,1,...,9 */
             my_spin = 2*j - 1;
             sum_nei = 2*i - 4;
             d_E = 2.*(J * my_spin * sum_nei + H * my_spin);
             x = exp(-d_E/T);
             prob[index] = x/(1.+x);
            /* printf("prob[%d]=%f\n",index,prob[index]); */
            };

    /* initialize local times */
    for (i = 0; i < M; i++)
        for (j = 0; j < M; j++)
            time[i][j]=0.;
}
```

```

/* initialize spins at random, in seedran(seed,b), b is dummy*/
seedran(31234,1);
for (i = 0; i < M*A; i++)
    for (j = 0; j < M*A; j++) {
        bit = 2*frand(1);          /* bit becomes 0 or 1 */
        spin[i][j] = 2*bit - 1;    /* spin becomes -1 or 1 */
/*      printf("spin[%d][%d]=%d\n",i,j,spin[i][j]);      */
    };

/* in the following loop single PE spawns nPEs other PEs for concurrent
   execution. Each child PE would execute subroutine work(my_id) with its
   own argument my_id. */

for (child_id = 0; child_id < nPEs; child_id++)
    if (fork() == 0) {
        tmp_affinity(child_id);    /* fixing a PE for process child_id */
        work(child_id);            /* starting a child PE process */
        exit(0);
    }

/* in the following loop the parent PE awaits termination of each child PE
   then terminates itself */
for (child_id = 0; child_id < nPEs; child_id++) wait(0);
exit(0);
}

work(my_id)
int my_id;
{
    int i,j;
    int coord, var;
    int x,y,my_i,my_j,sum_nei, nei_i,nei_j;
    int up_i, down_i, left_j, right_j;
    int i_base, j_base;
    int index;
    double frand();
    double r;
    double end_time;

    end_time = END_TIME*A*A;
/*normalizing time scale for multiprocessor execution*/

```



```

my_i = my_id%M;          /*PE my_id carries small square (my_i,my_j)*/
i_base = my_i*A;
up_i = (my_i + 1)%M;
down_i = (my_i + M - 1)%M;

my_j = (my_id-my_i)/M;
j_base = my_j*A;
left_j = (my_j + M - 1)%M;
right_j = (my_j + 1)%M;

seedran(my_id*my_id*my_id,my_id);
/*PE my_id has its own copy of pseudo-random number generator and initializes it
   using seedran(seed,my_id) with unique seed=my_id*my_id*my_id */

while(time[my_i][my_j] < end_time)
{
  r = frand(my_id);
  /*PE my_id obtains next pseudo-random number from its own sequence*/
  x = r*A;
  y = (r*A-x)*A;
  /*pick a random cell with internal address (x,y) within the A*A square*/

/*compute sum of neighboring spins*/
  sum_nei = 0;
  for (coord = 0; coord < 2; coord += 1)
    for (var = -1; var < 2; var += 2)
    {
      nei_i = x;
      nei_j = y;
      if(coord == 0) nei_i += var;
      if(coord == 1) nei_j += var;

      if(0 <= nei_i && nei_i < A && 0 <= nei_j && nei_j < A)
      {
        nei_i += i_base;
        nei_j += j_base;
      }
      else
      {
        /* 4 possible reasons to wait for a neighboring PE */
        if(-1 == nei_i) while (time[down_i][my_j] < time[my_i][my_j]) ;
        if(-1 == nei_j) while (time[my_i][left_j] < time[my_i][my_j]) ;
        if(nei_i == A) while (time[up_i][my_j] < time[my_i][my_j]) ;
        if(nei_j == A) while (time[my_i][right_j] < time[my_i][my_j]) ;
      }
    }
}

```

```

        nei_i = (nei_i+i_base+am)%am;
        nei_j = (nei_j+j_base+am)%am;
    };
    sum_nei += spin[nei_i][nei_j];
};

/*recover index*/
index = (sum_nei + 4)/2 + 5*(spin[x+i_base][y+j_base] + 1)/2;

r = frand(my_id);

if(r < probab[index])
    spin[x+i_base][y+j_base] *= -1;
else /* printf(": NO flip\n") */ ;

r = frand(my_id);
time[my_i][my_j] += -log(r);
};
}

```